JOURNAL OF BACTERIOLOGY, June 2002, p. 2889–2897 Vol. 184, No. 11
0021-9193/02/$04.00+0 DOI: 10.1128/JB.184.11.2889–2897.2002

Identification of a Lycopene β-Cyclase Required for Bacteriorhodopsin Biogenesis in the Archaeon *Halobacterium salinarum*

Ronald F. Peck,[1]† Eric A. Johnson,[2] and Mark P. Krebs[1]*

Department of Biomolecular Chemistry, University of Wisconsin Medical School,[1] and Department of Food Microbiology and Toxicology and Department of Bacteriology,[2] University of Wisconsin, Madison, Wisconsin 53706

Received 10 January 2002/Accepted 8 March 2002

Biogenesis of the light-driven proton pump bacteriorhodopsin in the archaeon *Halobacterium salinarum* requires coordinate synthesis of the bacterioopsin apoprotein and carotenoid precursors of retinal, which serves as a covalently bound cofactor. As a step towards elucidating the mechanism and regulation of carotenoid metabolism during bacteriorhodopsin biogenesis, we have identified an *H. salinarum* gene required for conversion of lycopene to β-carotene, a retinal precursor. The gene, designated *crtY*, is predicted to encode an integral membrane protein homologous to lycopene β-cyclases identified in bacteria and fungi. To test *crtY* function, we constructed *H. salinarum* strains with in-frame deletions in the gene. In the deletion strains, bacteriorhodopsin, retinal, and β-carotene were undetectable, whereas lycopene accumulated to high levels (≈1.3 nmol/mg of total cell protein). Heterologous expression of *H. salinarum crtY* in a lycopene-producing *Escherichia coli* strain resulted in β-carotene production. These results indicate that *H. salinarum crtY* encodes a functional lycopene β-cyclase required for bacteriorhodopsin biogenesis. Comparative sequence analysis yields a topological model of the protein and provides a plausible evolutionary connection between heterodimeric lycopene cyclases in bacteria and bifunctional lycopene cyclase-phytoene synthases in fungi.

Microbial rhodopsins consist of a covalent complex between an opsin, containing seven transmembrane α-helices, and retinal, a light-sensitive cofactor. Members of the microbial rhodopsin family were first identified in the archaea, but examples have been found recently in fungi and marine proteobacteria (35). Archaeal rhodopsins act as light-driven ion transporters and phototaxis receptors, and they share a common reaction mechanism in which the primary event is photoisomerization of retinal from an all-*trans* to a 13-*cis* configuration (27, 35). Fungal and bacterial rhodopsins are thought to function in the same way as archaeal rhodopsins, based on similarities in their photochemistry and ion transport properties (4, 5, 7, 35). Although the functional properties of microbial rhodopsins have been characterized extensively, relatively little is known about their biogenesis.

We have studied the biogenesis of a well-characterized member of the microbial rhodopsin family, bacteriorhodopsin (BR). BR is produced by the archaeon *Halobacterium salinarum* from bacterioopsin (BO) and carotenoids, which are synthesized by the organism and converted to retinal, which forms a covalent linkage with BO. BR is the most abundant of four rhodopsins produced by *H. salinarum,* which also include halorhodopsin and sensory rhodopsins I and II (27, 35). Studying the biogenesis of BR and other rhodopsins in *H. salinarum* is attractive because molecular genetic tools are available, including transformation (11), selectable markers (16, 24), and targeted gene replacement (29). Significantly, the genome sequence of a closely related organism, *Halobacterium* sp. strain NRC-1, has been determined (26), so functional genomic approaches are possible. BR production in *H. salinarum* has been used as a model for several steps in membrane protein biogenesis, such as protein insertion into the membrane (12, 13), biosynthesis and assembly of membrane-bound cofactors (30), and assembly of protein-lipid complexes (17, 18, 20).

In studies of cofactor assembly during BR biogenesis, we have focused on identifying cellular factors that participate in the biosynthesis and metabolism of carotenoids and are required for BR production. A pathway for retinal biosynthesis in archaeal halophiles closely related to *H. salinarum* has been proposed based on chemical inhibition studies, the in vitro conversion of isoprenoid precursors to the C_{40} carotenoid β-carotene, and the carotenoid biosynthetic pathways of other organisms (23, 37). In this pathway (Fig. 1), a series of condensation reactions among isoprenoids of various lengths leads to formation of the C_{40} carotenoid, phytoene. Phytoene then undergoes four desaturation reactions to yield lycopene. Both ends of lycopene are then cyclized to form β-carotene, which is thought to serve as the immediate precursor of retinal.

We previously identified two genes, *brp* and *blh*, that are required for generating BR from BO and carotenoid in *H. salinarum* (30). The *brp* gene was discovered in earlier studies of spontaneous insertion mutations that abolished BR production (6), but a precise role of the gene could not be ascertained because of transcriptional polar effects of insertions in *brp* (30). The *blh* gene was identified as a paralog of *brp* by sequence analysis of the *Halobacterium* sp. NRC-1 genome (30). Deletion of both *brp* and *blh* abolished BR production and led to the accumulation of β-carotene, suggesting that these genes encode proteins that catalyze the conversion of β-carotene to retinal (30). *brp* and *blh* were the first genes found to be required for the assembly of a microbial rhodopsin from carotenoids and a microbial opsin.

In the work reported here, we have identified a third carot-

* Corresponding author. Present address: Department of Biological Sciences, Illinois State University, Normal, IL 61790. Phone: (309) 438-3834. Fax: (309) 438-3722. E-mail: mpkrebs@ilstu.edu.

† Present address: Department of Medical Microbiology and Immunology, University of Wisconsin Medical School, Madison, WI 53706.

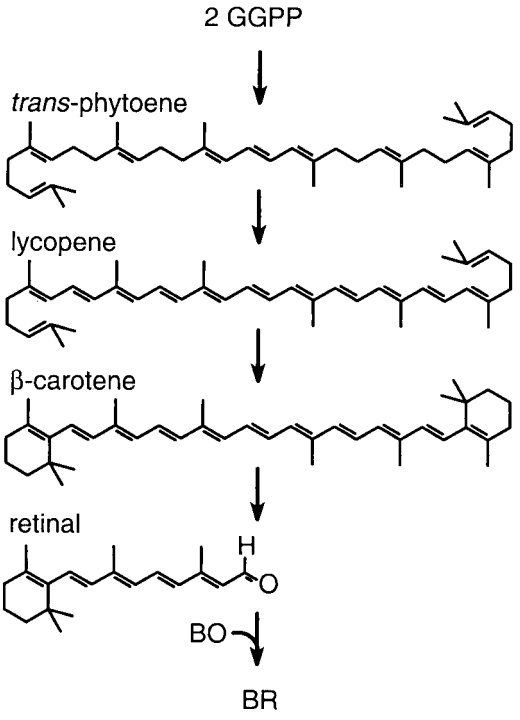

FIG. 1. Proposed carotenoid metabolic pathway leading to BR formation. Geranylgeranyl pyrophosphate (GGPP) is a C_{20} isoprenoid precursor of phytoene. Partially desaturated intermediates in the conversion of *trans*-phytoene to lycopene are not shown. The reactions that generate BR from β-carotene and BO are unknown but are proposed to include a symmetric oxidative cleavage followed by binding of retinal to BO.

enoid metabolic gene required for BR biogenesis. We searched for a lycopene cyclase gene because the conversion of lycopene to β-carotene is thought to be a key regulatory step in BR biogenesis (15). We identified a gene in *H. salinarum*, designated *crtY*, that encodes a protein homologous to a recently discovered class of lycopene cyclases found in both bacteria (22, 41) and fungi (2, 39, 40). Deletion studies of *crtY* in *H. salinarum* and heterologous expression studies in *Escherichia coli* indicate that the gene encodes a lycopene β-cyclase required for synthesizing β-carotene during BR production. The implications of these findings for BR biogenesis in *H. salinarum* and the evolution of lycopene cyclases are discussed.

MATERIALS AND METHODS

Materials. Oligonucleotides were obtained from Operon (Alameda, Calif.), *Taq* polymerase was obtained from Promega (Madison, Wis.), and restriction endonucleases and ligase were obtained from New England Biolabs (Beverly, Mass.). Lycopene, β-carotene, and retinal were obtained from Sigma.

Plasmid construction. Plasmids used in this study are listed in Table 1. Plasmids were propagated in the *E. coli* strain DH5α except where noted. A plasmid suitable for general gene replacement was constructed by combining the 5.1-kb *Kpn*I-*Eco*RI fragment of pMPK85 (17) with the 1.4-kb *Kpn*I-*Eco*RI fragment from pMPK408 (29). The resulting plasmid, pMPK428, contains a mevinolin resistance determinant, the *ura3* cassette, a polylinker site, and features to allow propagation in *E. coli*. Two-step PCR was used to construct the Δ*crtY* plasmids. As a first step, reactions were carried out with the primer pairs 1 (TCTAGATCTAGATGAACCGTGATCTGAACAGC) and 2 (GTGCTCGATCTCGATCTCGACAGCCAGGAACGTGAGGT) or 3 (GAGATCGAGATCGAGCAGCAGTACACCACCGGAATCAC) and 4 (AAGCTTAAGCTTACCCACAACAGGAGGGTTTC), using MPK1 (19) genomic DNA as template. The PCR products were used as template in the second PCR step with the primers 1 and 4, yielding a 1.5-kb product with two *Xba*I sites at the 5′ end and two *Hin*dIII sites at the 3′ end of the fragment (restriction sites underlined in the primer sequences). The sites were duplicated to increase restriction efficiency. The PCR product was fully digested with *Xba*I and *Hin*dIII and combined with the 6.5-kb *Xba*I-*Hin*dIII fragment from pMPK428 to yield pMPK430. This plasmid harbors a 1.5-kb section of DNA homologous to the *H. salinarum* chromosome with an in-frame *crtY* deletion of 555 bp and an 18-bp insertion at the deletion site. pMPK431, a similar plasmid that harbors an in-frame *crtY* deletion of 228 bp with an 18-bp insertion at the deletion site, was constructed by the same strategy except that the primers 1 and 5 (GTGCTCGATCTCGATCTCCTGCGTGATGACGAACAGAT) and 3 and 4 were used in the first PCR step. To create a complementation strain containing *crtY* at the *ura3* locus, PCR was carried out with the primers 1 and 6 (AGATCTAGATCTAAAAGCCGCGCCGGTTCAACGCCACCGGGCTAGCA) by using MPK1 genomic DNA as template. The resulting product contained the *crtY* gene and flanking DNA with *Xba*I and *Bgl*II sites introduced in the primers. The PCR product was digested with *Xba*I and *Bgl*II and ligated into the *Xba*I-*Bgl*II fragment of pMPK424, which contains the mevinolin resistance determinant, the *ura3* cassette, and features to allow propagation in *E. coli* (30). pMPK424 was prepared from a methylation-deficient strain (CSH26 *dam*). The resulting plasmid, pMPK432, contains the *crtY* open reading frame, 605 bp of upstream flanking sequence to allow normal transcription, and a 21-bp sequence derived from the *bop* transcription terminator (14) to ensure the transcription termination of *crtY*.

To create a lycopene-producing strain of *E. coli*, the plasmid pACCAR16Δ*crtX* (25) (provided by J. von Lintig) was modified. This plasmid contains four functional *Erwinia uredovora* genes that result in β-carotene production. The plasmid was partially digested with *Bst*XI, which cuts twice within the *E. uredovora crtY* gene, and self-ligated after trimming the 3′ overhangs with the large Klenow fragment of DNA polymerase I (New England Biolabs). The ligated sample was then transformed into *E. coli* JM109, and pink colonies were obtained at a

TABLE 1. Microbial strains and plasmids

Strain or plasmid	Relevant characteristic(s)	Source or reference
Strains		
MPK1	*H. salinarum* Rub$^-$ Vac$^-$	19
MPK407	MPK1 Δ*ura3*	29
MPK426	MPK407 Δ*crtY* (codons 45 to 229)	This study
MPK427	MPK407 Δ*crtY* (codons 121 to 229)	This study
MPK428	MPK426 *ura3*::*crtY*	This study
Plasmids		
pACCAR16 Δ*crtX*	pACYC-based plasmid containing *E. uredovora* carotenogenic genes	25
pBAD TOPO TA	pUC-based expression vector with arabinose-inducible promoter	Invitrogen
pMPK85	pAT153-based plasmid containing mevinolin resistance determinant (Mev^r)	17
pMPK408	Litmus 28 (NEB)-based plasmid containing *ura3*	29
pMPK424	pAT153-based plasmid containing Mev^r *ura3*, and unique *Xba*I, *Bgl*II sites flanked by 2.0-kb *ura3* flanking sequence	30
pMPK428	1.4-kbp *Kpn*I-*Eco*RI *ura3* fragment of pMPK408 combined with 5.1-kbp *Kpn*I-*Eco*RIpAT153, Mev^r fragment of pMPK85	This study
pMPK430	Δ*crtY* (codons 45 to 229) PCR fragment in pMPK428	This study
pMPK431	Δ*crtY* (codons 121 to 229) PCR fragment in pMPK428	This study
pMPK432	1.4-kbp *Xba*I-*Bgl*II *crtY* PCR fragment in pMPK424	This study
pMPK434	Partial *Bst*XI digest of pACCAR16Δ*crtX*, recircularized	This study
pMPK438	*crtY* open reading frame in pBAD TOPO TA vector	This study
pMPK454	pBAD TOPO TA vector, circularized	This study

frequency of ≈0.5%. The deletion junction in *crtY* in the resulting plasmid, pMPK434, was verified in one isolate. This plasmid was found by UV-visible spectroscopy to promote lycopene production without promoting β-carotene production. To construct an expression vector for *H. salinarum crtY*, the primers GTGGCGTGTCCGACTCGACA and TCAACGCCACCGGGCTAGCA were used in a PCR with MPK1 genomic DNA as template. The PCR product was cloned directly into the pBAD TOPO TA expression vector (Invitrogen, Carlsbad, Calif.), and the resulting plasmid, pMPK438, was transformed into *E. coli* JM109 with pMPK434. To obtain a control strain containing only the expression vector, the pBAD TOPO TA vector was self-ligated to make pMPK454 and introduced into pMPK434-containing *E. coli* JM109.

***H. salinarum* strain construction.** *H. salinarum* strains (Table 1) were obtained by using a two-step *ura3*-based gene replacement method as described previously (29). Briefly, strains were transformed as described elsewhere (19) with selection for mevinolin resistance and then replated on medium containing 5-fluoroorotic acid to select for recombinants. Colonies resistant to 5-fluoroorotic acid were screened by PCR to identify the desired recombinants. The Δ*crtY* strain lacking codons 45 to 229, MPK426, was isolated by transforming pMPK430 into MPK407 (29). The Δ*crtY* strain lacking codons 121 to 229, MPK427, was isolated by transforming pMPK431 into MPK407. The complementation strain with *crtY* integrated at the *ura3* locus, MPK428, was isolated by transforming pMPK432 into MPK426. For all strains, recombinants resistant to 5-fluoroorotic acid were obtained at a frequency of ≈1:100, of which 1 to 20% had the desired gene replacement. The structures of the *bop*, *brp*, *blh*, *crtY*, and *ura3* loci were confirmed in all strains by PCR and Southern blot analysis as described previously (19). The sequences of the entire deleted *crtY* open reading frame of MPK426 and the deletion junction within the *crtY* open reading frame in MPK427 were confirmed by ABI PRISM Big Dye Primer Cycle sequencing (Applied Biosystems, Inc., Foster City, Calif.) by using various primers. Sequencing reactions were analyzed with a 337XL automated DNA sequencer (Applied Biosystems, Inc.) at the University of Wisconsin Biotechnology Center.

Quantitation of BR, BO, and carotenoids in *H. salinarum*. *H. salinarum* strains were grown under conditions to induce BR synthesis, cell lysates were prepared, and BR and BO levels were measured as described elsewhere (30), except that cultures were incubated for 86 to 90 h. Total carotenoid was extracted from cell lysates as described previously (15), except that lysates were illuminated for 3 min with a >520-nm light prior to extraction to convert all retinal to the all-*trans* isomer.

To identify the major carotenoid in Δ*crtY* strains, the extracts were fractionated by high-performance liquid chromatography (HPLC) on an HPLX solvent delivery system (Rainin Instrument Co., Inc., Emeryville, Calif.) coupled with a reverse-phase Alltech Altima C_{18} column (250 by 4.6 mm; 5 μm particle size) (Alltech Associates, Inc., Deerfield, Ill.) and an Alltech Econosphere C_{18} 5-μm guard column. The mobile phase was a gradient of solvent A (85% acetonitrile, 15% methanol) and solvent B (dichloromethane) eluting at 1 ml/min. The solvent change over a 25-min sample run was programmed as follows: elution with 100% solvent A, 1 min; gradient to 32% solvent B, 1.5 min; isocratic elution with solvent B, 5.5 min; gradient to 65% solvent B, 0.5 min; isocratic elution with solvent B, 6 min; gradient to 100% solvent A, 0.5 min; and reequilibration with 100% solvent A, 4 min. The eluate was monitored at 380 nm for the first 8 min and at 474 nm for the remainder of each run with a Dynamax UV-1 variable wavelength UV-visible absorbance detector (Rainin Instrument Co., Inc.). HPLC fractions eluting at ≈11 min were collected and evaporated under nitrogen gas. The UV-visible spectrum was obtained by dissolving the sample in hexane and scanning on a Perkin-Elmer λ2 Spectrophotometer (Applied Biosystems, Inc.). For mass spectrometry analysis, an aliquot of the sample was evaporated to dryness and resuspended in acetone to a lycopene concentration of 10 μM. Mass spectrometry was performed at the University of Wisconsin Biotechnology Center on a Bruker Biflex III matrix-assisted laser desorption ionization–time of flight (MALDI-TOF) instrument (Bruker Analytical Systems, Billerica, Mass.) using 2,5-dihydrobenzoic acid as a matrix.

Simultaneous measurement of retinal, β-carotene, and lycopene was carried out using the HPLC conditions described above. Standard curves were generated with commercial all-*trans* retinal, β-carotene, and lycopene. The efficiency of extraction of retinal was approximately 55% as judged by parallel extractions of purified BR (data not shown). The difference in retinal yields between this study and our earlier results (30) is likely due to a more accurate standard curve generated by using freshly obtained retinal.

Extraction and analysis of carotenoids in *E. coli*. To analyze carotenoid production in *E. coli*, Luria-Bertani medium (50 ml in a 125-ml Erlenmeyer flask) containing chloramphenicol (170 μg/ml) and ampicillin (150 μg/ml) was inoculated with 1 ml of overnight culture grown in the same medium to saturation. Cultures were grown in the dark at 28°C with shaking at 250 rpm for approximately 4 h to an optical density at 600 nm (OD_{600}) of ≈0.5. Cells were then induced by the addition of 0.5 ml of 20% arabinose to a final concentration of 0.2% arabinose. Cultures were removed at 0, 3, and 6 h after induction and cells were harvested by centrifuging at 6,000 × *g* for 20 min at 4°C. The cell pellet was resuspended in 50 ml of 50 mM Tris-Cl (pH 8.0) and centrifuged again at 6,000 × *g* for 20 min, followed by a brief centrifugation to remove all traces of the supernatant. The cell pellet was then resuspended in 3 ml of Tris-Cl buffer followed by vigorous vortexing to obtain a homogenous suspension. A 2.5-ml aliquot of the cell suspension was added to 22.5 ml of acetone and the mixture was stirred vigorously for 20 min. Twelve milliliters of hexane-water (4:1) was added to the mixture, which was then stirred for 2 min, poured into a 100-ml graduated cylinder, and allowed to settle for 5 min. The upper layer containing the carotenoids was then removed and evaporated to dryness under nitrogen. The remaining 0.5 ml of the cell suspension was solubilized in electrophoresis sample buffer, and total cell protein was measured by a bicinchoninic acid assay (Pierce, Rockford, Ill.).

The carotenoid extracts were analyzed and quantified using the same HPLC method described above, except that the eluate was monitored at 474 nm throughout the run. To confirm that β-carotene was synthesized in *E. coli* strains expressing *H. salinarum crtY*, fractions eluting at ≈13 min were collected, evaporated to dryness under nitrogen, resuspended in isopropanol, and scanned to obtain UV-visible spectra. Aliquots of the β-carotene sample were prepared, and mass spectrometry analysis was performed as described above.

RESULTS

Sequence identification of *Halobacterium* sp. NRC-1 *crtY*. In the initial annotation of the *Halobacterium* sp. NRC-1 genome sequence (26), BLAST analyses (1) with the National Center for Biotechnology Information sequence database using known plant (LCYB-like or CrtL-like) and bacterial (CrtY-like) lycopene β-cyclases yielded no promising candidates. However, subsequent BLAST searches revealed a single gene encoding a putative membrane protein homologous to members of a newly discovered class of heterodimeric CrtYc and CrtYd lycopene β-cyclases in bacteria (22, 41) and bifunctional lycopene cyclase-phytoene synthases in fungi (2, 39, 40). This gene had been assigned as encoding a 162-amino-acid protein (Fig. 2, Ha, ampersand) corresponding to geranylgeranyl transferase (26), but this function now appears unlikely. Further analysis indicated that the encoded protein is longer at the N terminus than initially assigned, taking codon third-position GC bias into account (data not shown) and allowing for the use of GUG as a start codon. Two potential GUG codons are upstream of the assigned start, yielding a protein of 237 amino acids (Fig. 2, Ha, asterisk) or 270 amino acids (Fig. 2, full-length Ha protein).

The predicted *Halobacterium* sp. NRC-1 *crtY* gene product aligns well with bacterial and fungal enzymes that possess lycopene cyclase activity (Fig. 2, Xd, Pb, Mc, Blc, Bld, Mac, and Mad). The similarity extends to orthologs of these proteins predicted from the nucleotide sequences of other carotenogenic organisms, including the archaeon *Sulfolobus solfataricus,* the fungus *Neurospora crassa,* and the bacterium *Myxococcus xanthus* (Fig. 2, Ss, Nc, Mx7, and Mx8). The bacterial proteins are thought to act as a heterodimer of two closely related monomers, CrtYc and CrtYd (22, 41). In the bifunctional CrtYB proteins of fungi, two domains homologous to the bacterial proteins are fused to form an N-terminal lycopene cyclase domain, which in turn is fused to a C-terminal phytoene synthase domain (2, 39, 40). *Halobacterium* sp. NRC-1 CrtY is similar to the N-terminal domain of CrtYB. The polypeptide includes two homologous domains (34% identity over 101 amino acids) related to the monomeric bac-

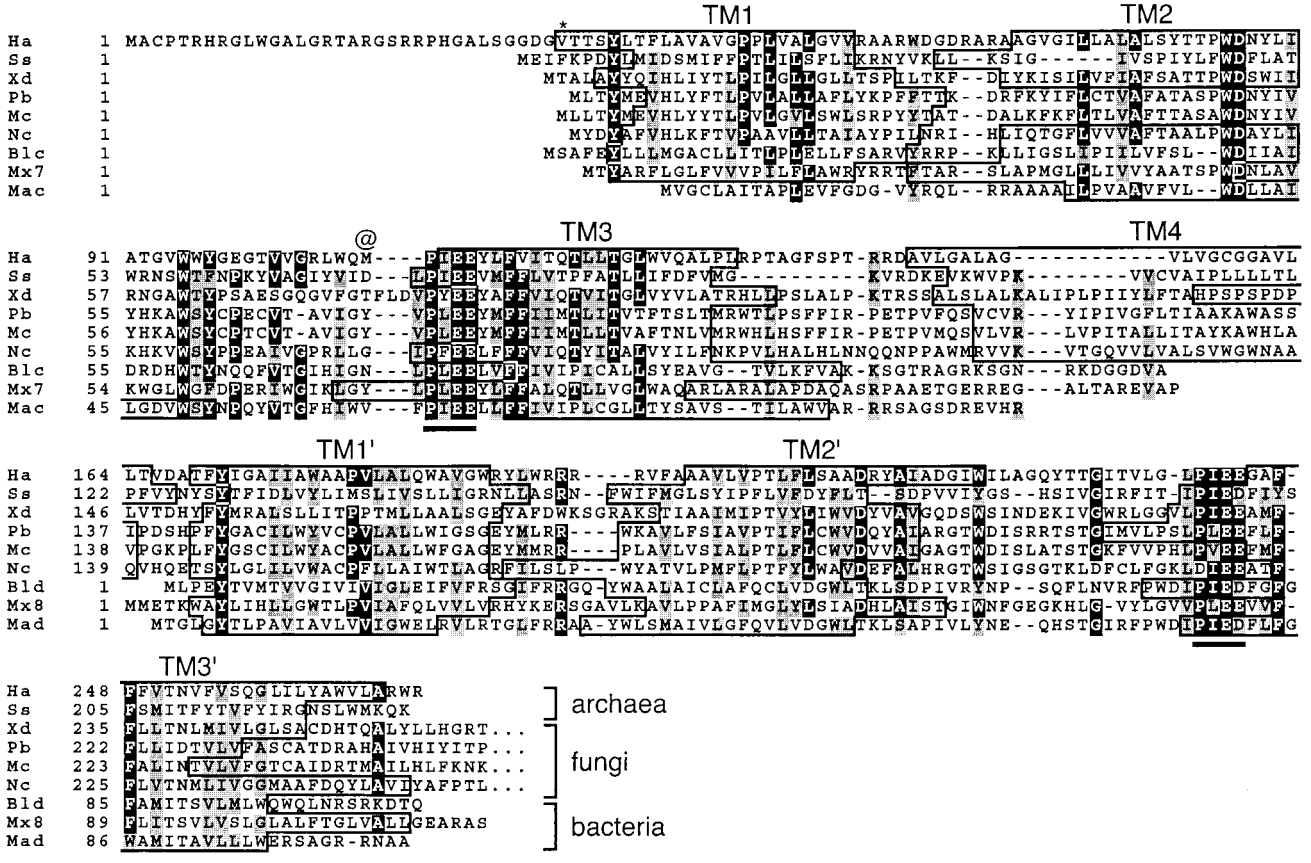

FIG. 2. Alignment of lycopene cyclases. Ha, *Halobacterium* sp. NRC-1 CrtY; Ss, the predicted CrtY ortholog from *S. solfataricus* (33); Xd, the CrtY portion of CrtYB from *Xanthophyllomyces dendrorhous* (40); Pb, the CarR portion of CarRA from *P. blakesleeanus* (2); Mc, the CarR portion of CarRP from *M. circinelloides* (39); Nc, the CrtY portion of the predicted CrtYB from *N. crassa* (32); Blc and Bld, the heterodimeric lycopene cyclase proteins CrtYc and crtYd from *Brevibacterium linens* (22); Mx7 and Mx8, the predicted proteins encoded by open reading frames 7 and 8 in the carotenogenic gene cluster of *M. xanthus* (9); Mac and Mad, CrtYc and CrtYd from *M. aurum* (41). Sequences of the heterodimeric proteins were artificially fused for alignment. Sequence alignment was obtained through the use of the software program ClustalW (38). Identical residues are highlighted in black and similar residues are shaded in gray. A possible alternate N terminus in *Halobacterium* sp. NRC-1 is denoted by an asterisk, and the initially assigned N terminus is denoted by the @ symbol. The conserved PxE(E/D) motif previously found to be required for lycopene cyclase activity (2) is underlined. The boundaries of transmembrane segments (TM) predicted by TMHMM (21) are boxed.

terial enzymes (Fig. 2). Each domain contains the highly conserved PXE(E/D) motif that is present in all members of this class of lycopene cyclases (Fig. 2) and is required for catalytic activity of the *Phycomyces blakesleeanus* enzyme (2).

The structural similarity of *Halobacterium* sp. NRC-1 CrtY to other lycopene cyclases is reinforced by comparing their membrane topology (Fig. 2) as computed by TMHMM (21). The bacterial CrtYcs and CrtYds are predicted to contain three transmembrane segments (Fig. 2, TM1 to -3 and TM1′ to -3′, respectively), which are also evident in the repeated domains of the fungal and *Halobacterium* sp. NRC-1 proteins. A fourth transmembrane helix links the repeated domains of the fungal and archaeal proteins (Fig. 2, TM4). (TM1 was not identified in the *Mycobacterium aurum* CrtYc sequence but was predicted when 14 additional N-terminal residues from an upstream GUG start were included [data not shown]. TM2 was not identified in the *P. blakesleeanus* and *Mucor circinelloides* proteins, but significant peaks in the TM2 region were apparent in hydropathy plots generated by TMHMM [21].)

The identification of *Halobacterium* sp. NRC-1 *crtY* is also supported by the proximity of the gene to *blh*, which appears to partially substitute for *brp* function in retinal biosynthesis during BR production (30). The *crtY* gene is directly upstream of *blh*, and their open reading frames are predicted to overlap by eight codons (data not shown), based on the putative start codon of *blh* (30). This arrangement raises the possibility that the genes are translationally coupled in an operon and that the gene products are involved in the same metabolic process. Thus, sequence similarity, predicted topology, and gene arrangement suggest that *Halobacterium* sp. NRC-1 *crtY* encodes a lycopene β-cyclase required for BR biogenesis.

Deletion of *crtY* eliminates BR expression. Genetic analysis was required to determine whether the *crtY* gene encodes a functional product and whether the putative lycopene β-cyclase is required for the synthesis of the retinal cofactor of BR. We used *H. salinarum* as a strain for genetic analysis because all of our previous work on BR biogenesis has been performed in this strain. The strains used in our laboratory are derived from *H. salinarum* R1 (19), which was isolated from *Halobacterium* sp. NRC-1 (31). We have found very few differences between the two organisms among several genes sequenced in our laboratory, including *brp, ura3*, and *secY*, and among a

subset of genes available from the two organisms at the National Center for Biotechnology Information (unpublished results). Thus, use of the *Halobacterium* sp. NRC-1 genome sequence for analysis of *H. salinarum* is valid.

To examine the role of *crtY* in *H. salinarum,* two Δ*crtY* strains were constructed. MPK426 has a deletion of codons 45 to 229 of the proposed full-length open reading frame. MPK427 has a deletion of codons 121 to 229 that was designed to minimize possible polar effects on *blh* transcription. Such effects might occur if transcriptional signals near the 5′ end of the gene were deleted. Colonies from both Δ*crtY* strains were pale red and distinct from the purple color of the wild type. This result suggested that BR production in the Δ*crtY* strains was reduced due to the loss of *crtY*.

To accurately measure BR levels, cells were grown under microaerobic conditions known to induce BR synthesis (28). Cultures were grown in the dark to prevent differences in BR levels from affecting cell energy states. Cell lysates from the Δ*crtY* strains lacked BR, as shown by the absence of the BR peak at 570 nm (Fig. 3A). As measured by light-dark difference spectroscopy (19), BR represented ≈4% of total cell protein in the wild-type strain but was undetectable in both Δ*crtY* strains (Fig. 3B and 4). Levels of BO were only slightly reduced (Fig. 3A, insert, and 4), as determined by immunoblotting with a BO C-terminal antibody. The slight reduction in BO could not account for the complete elimination of BR synthesis in Δ*crtY* strains. The absence of BR without a significant reduction in the levels of apoprotein BO suggests that the loss of *crtY* results in a defect in the synthesis of the BR retinal cofactor.

Δ*crtY* strains accumulate lycopene and do not synthesize β-carotene or retinal. In addition to lacking a characteristic BR peak, spectra of Δ*crtY* cell lysates exhibited a sharp peak at ≈340 nm that was absent from that of the wild type (Fig. 3A). A similar peak in cell lysate spectra from a *Halobacterium* sp. strain lacking synthesis of C_{50} carotenoids had been attributed to an accumulation of lycopene (37), which has an absorbance maximum near 340 nm in aqueous environments that is attributed to aggregation (10, 37). To examine the possibility that lycopene had accumulated in the Δ*crtY* strains, Δ*crtY* and wild-type lysates were extracted with acetone and hexane to recover carotenoids and retinal (15) and fractionated by HPLC to quantify lycopene, β-carotene, and retinal. The Δ*crtY* extracts exhibited a major component eluting at 11.1 min that comigrated with commercial lycopene (Fig. 5A, trace 2). This peak was not detected in the wild-type extract (Fig. 5A, trace 1). To confirm that this major carotenoid species was lycopene, peak HPLC fractions from both Δ*crtY* strains were collected and compared with commercial lycopene. The UV-visible spectra in hexane were similar, with both Δ*crtY* extracts and commercial lycopene having absorption maxima at 470 nm (Fig. 5B). MALDI-TOF mass spectrometry yielded mass ion values of 536.42 and 536.43 for the Δ*crtY* (MPK426) fraction and commercial lycopene, respectively. These results confirmed that lycopene is the major carotenoid accumulating in the Δ*crtY* strains.

The accumulation of lycopene in the Δ*crtY* strains was accompanied by a decrease of both β-carotene and retinal to undetectable levels (Fig. 5A, trace 2, and Fig. 4, samples 2 and 3). The simplest interpretation of these results is that *crtY* encodes a lycopene β-cyclase that catalyzes the conversion of lycopene to β-carotene, the precursor of the retinal cofactor of BR.

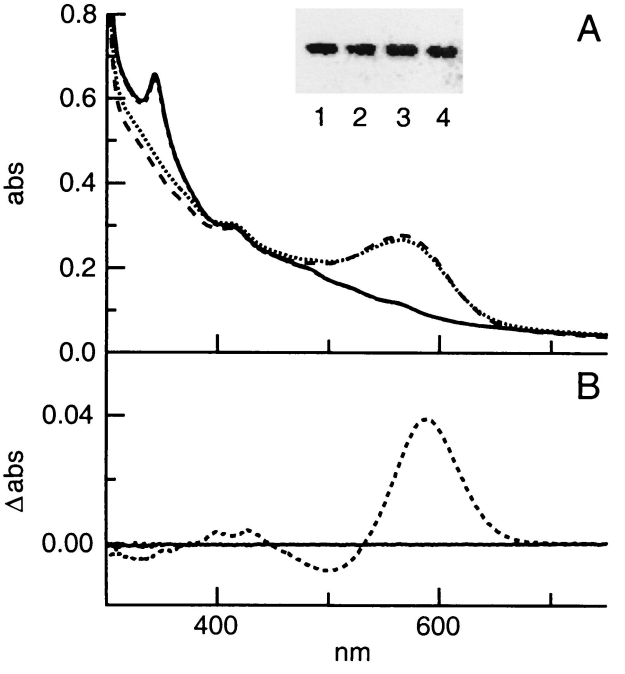

FIG. 3. (A) UV-visible spectra of cell lysates from wild-type (dotted line), Δ*crtY* (MPK426) (solid line), Δ*crtY* (MPK427) (dashed and dotted line), and Δ*crtY ura3*::*crtY* complementation (dashed line) strains. Cells were grown under microaerobic conditions to induce BR synthesis. Spectra of lysates were obtained at a total cell protein concentration of ≈3 mg/ml and normalized for slight differences in protein concentration. Inset, immunoblot of wild-type (lane 1), Δ*crtY* (MPK426) (lane 2), Δ*crtY* (MPK427) (lane 3), and Δ*crtY ura3*::*crtY* complementation (lane 4) lysates. Total cell protein (4.0 μg) was electrophoresed and immunoblotted with the C-terminal BR antibody, BR-114. The blot was analyzed by incubating with a fluorescein-conjugated secondary antibody and scanning with a fluoroimager. (B) Light-dark difference spectroscopy of wild-type (dotted line) and Δ*crtY* (MPK426) (solid line) lysates. Spectra were obtained from lysates dark-adapted for ≈12 h or light-adapted for 5 min. A light-dark difference spectrum was calculated, and the BR level was determined from the value at 587 nm. The estimated detection threshold is ≈1% of the wild-type level of BR.

ΔcrtY is complemented by an intact copy of *crtY*. To demonstrate that the Δ*crtY* phenotype was caused by the loss of *crtY* and not a polar effect on the downstream *blh* gene or a spurious mutation in an unknown gene, a complementation strain was constructed. The *crtY* open reading frame, flanked by 605 bp of upstream sequence to allow normal expression and regulation, was integrated at the *ura3* locus. The resulting strain, Δ*crtY ura3*::*crtY,* yielded purple colonies identical to those of the wild type. When grown under microaerobic conditions, BR, β-carotene, and retinal were restored to near wild-type levels and lycopene was undetectable (Fig. 3A; 4, sample 4; 5A, trace 3). As expected, BO levels were similar to those in the wild type (Fig. 3A, inset, and 4). The slight reduction in levels of BR, retinal, and β-carotene in the complementation strain may be due to a decrease in transcription or mRNA stability of *crtY* when expressed from a different locus. These results confirm that the Δ*crtY* phenotype is due solely to the loss of *crtY*.

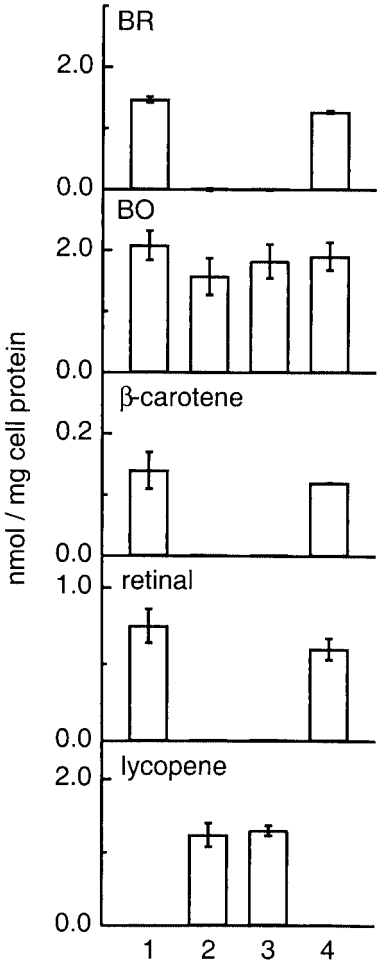

FIG. 4. Comparison of BR, BO, β-carotene, retinal, and lycopene levels in wild-type (sample 1), Δ*crtY* (MPK426) (sample 2), Δ*crtY* (MPK427) (sample 3), and Δ*crtY ura3*::*crtY* complementation (sample 4) strains. Cells were grown under microaerobic conditions to induce BR, and BR, BO, β-carotene, retinal, and lycopene levels were determined as described in Materials and Methods. All values are an average of three independent determinations and the error bars indicate 1 standard deviation.

Expression of *H. salinarum crtY* in lycopene-producing *E. coli* is sufficient to yield β-carotene. The experiments described above provide indirect evidence that the *H. salinarum crtY* encodes lycopene β-cyclase. To provide direct evidence that this is the case, the gene was introduced into an *E. coli* strain engineered to produce lycopene. The strain contains a pACYC derivative bearing carotenoid biosynthetic genes from *E. uredovora*. The *H. salinarum crtY* open reading frame was placed into a compatible pBAD expression vector to allow induction of *crtY* expression by arabinose. Upon induction, *E. coli* strains containing the *crtY* expression vector accumulated two carotenoid species which eluted at 12.5 and 13.2 min and were distinct from lycopene at 11.2 min (Fig. 6, 3 and 6 h traces).

To confirm that the major carotenoid species was β-carotene, the *E. coli* samples were extracted and fractionated by HPLC. The HPLC fractions corresponding to the peak at ≈13 min contained a species with UV-visible spectral features identical to commercial β-carotene, including an absorbance maximum of 450 nm in isopropanol (data not shown). MALDI-TOF mass spectrometry revealed that the extracted species had a mass ion value of 536.42, identical to that expected for β-carotene (30). Therefore, the major species synthesized in lycopene-producing *E. coli* when *H. salinarum crtY* is expressed is β-carotene. The minor species may be γ-carotene, which results from cyclization at one end of lycopene. A minor species of similar mobility relative to lycopene and β-carotene has been confirmed to be γ-carotene in studies of other lycopene cyclases in *E. coli* (22, 40).

β-Carotene was not detected in *E. coli* prior to inducing expression of *H. salinarum crtY* (Fig. 6, 0 h trace), and levels of

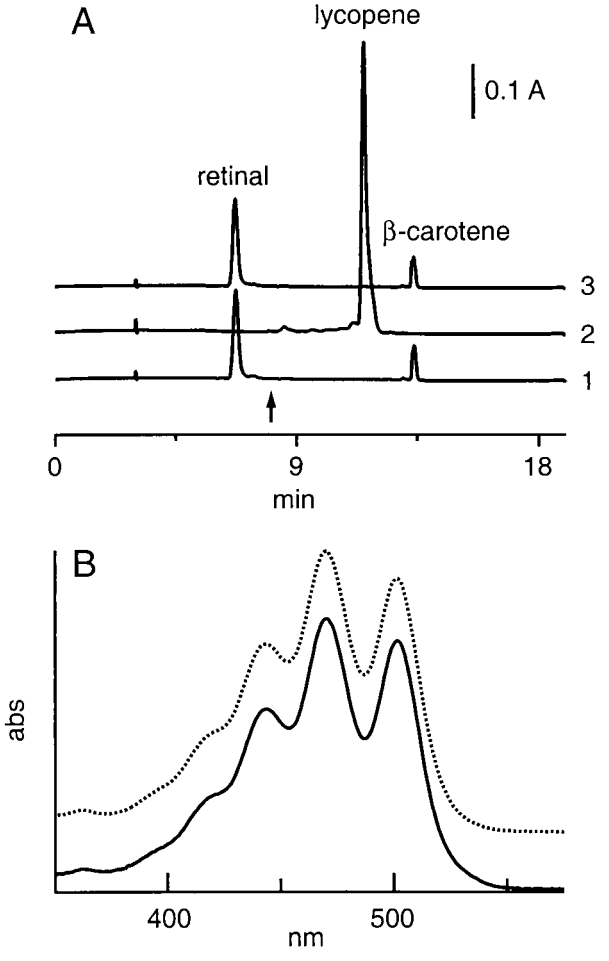

FIG. 5. (A) Comparison of lycopene, β-carotene, and retinal accumulation in the wild-type (trace 1), Δ*crtY* (MPK426) (trace 2) and Δ*crtY ura3*::*crtY* (trace 3) strains. Carotenoids were extracted from cells as described elsewhere (15) and analyzed by reverse-phase HPLC as described in Materials and Methods. At the time indicated by the arrow, the detector was switched from 380 nm, the wavelength at which retinal was quantified, to 474 nm to quantify lycopene and β-carotene. Traces are shown normalized to total cell protein and offset on the vertical axis for clarity. (B) UV-visible spectra of lycopene obtained from Δ*crtY* extract (solid line) and from a commercial source (dotted line). Total carotenoid was extracted from the Δ*crtY* strain MPK426 as described previously (15). Both *H. salinarum* extract and commercial lycopene were purified by reverse-phase HPLC as described in Materials and Methods, dissolved in hexane, and scanned on a Perkin-Elmer λ2 spectrophotometer. The absorbance scale is arbitrary, and spectra are offset on the vertical axis for clarity.

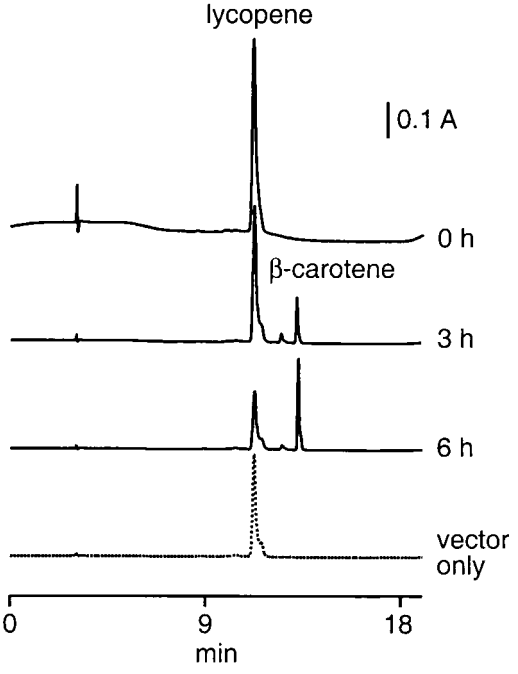

FIG. 6. Comparison of lycopene and β-carotene in lycopene-producing *E. coli* containing the pBAD expression vector only (dotted line) or harboring the *H. salinarum crtY* open reading frame (solid lines). Cells were grown to mid-log phase and expression was induced with the addition of arabinose to a concentration of 0.5%. Cells were harvested at 0, 3, or 6 h as indicated and total carotenoid was extracted and analyzed by HPLC as described in Materials and Methods. The vector-only sample was extracted 6 h after induction. Traces are shown normalized to total cell protein and offset along the vertical axis for clarity.

β-carotene were increased as the period of induction was prolonged (Fig. 6, 3 and 6 h traces). Moreover, a control strain containing the expression vector without the *H. salinarum crtY* insert did not produce β-carotene (Fig. 6, vector-only trace). These results demonstrate that conversion of lycopene to β-carotene in this strain is dependent on *crtY* expression and that the *H. salinarum crtY* encodes a functional lycopene β-cyclase.

DISCUSSION

We have identified an *H. salinarum* gene, *crtY*, that encodes a functional lycopene β-cyclase required for BR biogenesis. The function of the gene was tentatively assigned on the basis of similarities to recently identified lycopene β-cyclases found in fungi (2, 39, 40) and bacteria (22, 41). Our deletion analysis and heterologous expression studies of the gene confirmed this assignment.

Our results are consistent with a proposed carotenoid metabolic pathway in which lycopene is the immediate precursor of β-carotene, which in turn is a precursor of the retinal in BR. Several earlier experiments support this pathway. Inhibition of lycopene cyclization with nicotine leads to an increase in lycopene and a decrease in BR and retinal levels (37). β-Carotene production from lycopene is observed in cell-free lysates of *Halobacterium cutirubrum*, an extreme halophile closely related to *H. salinarum* (23). Finally, β-carotene accumulates when retinal and BR production is abolished by double deletion of *brp* and *blh* (30). Deletion of the *crtY* gene in the present study yielded results similar to those of the nicotine inhibition studies, except that the effects on BR and retinal levels were more pronounced. Thus, the proposed pathway for carotenoid metabolism during BR biogenesis is correct.

The step in this pathway catalyzed by CrtY may be the only means of synthesizing β-carotene in *H. salinarum*. First, a single *crtY* gene was identified in the *Halobacterium* sp. NRC-1 genome sequence. No orthologs of other lycopene cyclase genes were found. Second, deletion of the gene reduced the levels of β-carotene and BR to below detectable limits, indicating a complete block in β-carotene production. Third, the *crtY* deletion probably affects the synthesis of rhodopsins other than BR. In strains derived from *H. salinarum* S9, the levels of halorhodopsin and sensory rhodopsin I are ≈9% and ≈3% that of BR, respectively (8), and the level of sensory rhodopsin II is at least threefold lower than that of sensory rhodopsin I (34). Our strains lack the regulatory mutation in S9 (3) that leads to overproduction of BR, and possibly halorhodopsin and sensory rhodopsin I, but the ratio of these proteins is probably similar. If an alternative pathway existed to produce β-carotene for halorhodopsin, we would have detected a small retinal peak in the HPLC analysis of the Δ*crtY* extracts, which was not observed (Fig. 5A). Thus, it seems likely that the same pathway is used to synthesize β-carotene for both BR and halorhodopsin. We cannot exclude the possibility that the sensory rhodopsins use an alternative carotenoid metabolic pathway, since the very low amount of retinal from these proteins may have been undetected by our HPLC analysis.

Comparative sequence analysis and topology predictions provide a model for lycopene cyclase evolution. Evolutionary relationships among the bacterial and fungal proteins have been noted previously (2, 22, 40). The bacterial *crtYc* and *crtYd* genes may have arisen from duplication of a gene that encoded a homodimeric lycopene cyclase. Our topological analysis indicates that each monomer of the bacterial enzymes contains three transmembrane segments and has the same N-out–C-in orientation (Fig. 7). The conserved, potentially catalytic motif PXE(E/D) is thereby situated toward the extracytoplasmic face of the membrane in each monomer (Fig. 7). Archaeal CrtY proteins found in *H. salinarum* and predicted in *S. solfataricus* contain two domains similar to the bacterial proteins linked by an additional transmembrane segment that allows the topology of each domain to be retained (Fig. 7). The fungal *crtYB* gene appears to have arisen from fusion of an archaeal-like gene with a phytoene synthase (*crtB*) gene. The predicted membrane topology of fungal CrtYB is identical to that of the archaeal proteins and results in a cytosolic location for the phytoene synthase domain (Fig. 7), which is expected since the CrtB substrate geranylgeranyl pyrophosphate is generated in the cytosol. Thus, carotenogenic archaea encode a lycopene cyclase that has a structural organization intermediate between that of bacteria and fungi. Further studies may reveal whether the relationship among members of this class of cyclases arose from lateral gene transfer or evolution from a common ancestor.

H. salinarum CrtY and the related lycopene cyclases in bacteria and fungi may play a unique role in carotenoid metabolism. CrtY functions in the biogenesis of known integral mem-

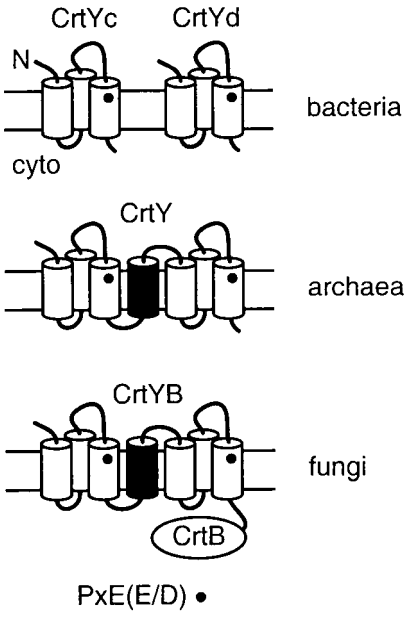

FIG. 7. Model of CrtY topology and evolutionary relatedness. Transmembrane helices are shown as cylinders and the lipid bilayer is indicated by parallel lines. The conserved catalytic motif PXE(E/D) is denoted by the dot (•). CrtB indicates the phytoene synthase domain of the fungal protein.

brane proteins, including BR and possibly other *H. salinarum* rhodopsins. Like CrtY, the other proteins implicated in *H. salinarum* BR biogenesis, including Brp and Blh, are predicted to be integral membrane proteins. Preliminary immunoblotting experiments of fractionated cells suggest that Brp is indeed localized to the *H. salinarum* membrane (M. P. Krebs, unpublished results). We propose that *H. salinarum* CrtY and related proteins are dedicated to producing β-carotene for use by other integral membrane proteins, such as Brp and Blh. Direct interaction of these proteins within the membrane may influence carotenoid and retinal metabolism during BR biogenesis in *H. salinarum,* which is known to be regulated (15, 36). Further experiments are in progress to test this model.

ACKNOWLEDGMENTS

We thank T. Bergsbaken for technical assistance and C. Echavarri-Erasun for help with HPLC.

This research was supported by National Science Foundation grant MCB-9983120 to M.P.K.

REFERENCES

1. **Altschul, S. F., T. L. Madden, A. A. Schäffer, J. Zhang, Z. Zhang, W. Miller, and D. J. Lipman.** 1997. Gapped BLAST and PSI-BLAST: a new generation of protein database search programs. Nucleic Acids Res. **25:**3389–3402.
2. **Arrach, N., R. Fernández-Martin, E. Cerdá-Olmedo, and J. Avalos.** 2001. A single gene for lycopene cyclase, phytoene synthase, and regulation of carotene biosynthesis in *Phycomyces*. Proc. Natl. Acad. Sci. USA **98:**1687–1692.
3. **Baliga, N. S., S. P. Kennedy, W. V. Ng, L. Hood, and S. DasSarma.** 2001. Genomic and genetic dissection of an archaeal regulon. Proc. Natl. Acad. Sci. USA **98:**2521–2525.
4. **Béjà, O., L. Aravind, E. V. Koonin, M. T. Suzuki, A. Hadd, L. P. Nguyen, S. B. Jovanovich, C. M. Gates, R. A. Feldman, J. L. Spudich, E. N. Spudich, and E. F. DeLong.** 2000. Bacterial rhodopsin: evidence for a new type of phototrophy in the sea. Science **289:**1902–1906.
5. **Béjà, O., E. N. Spudich, J. L. Spudich, M. Leclerc, and E. F. DeLong.** 2001. Proteorhodopsin phototrophy in the ocean. Nature **411:**786–789.
6. **Betlach, M., J. Friedman, H. W. Boyer, and F. Pfeifer.** 1984. Characterization of a halobacterial gene affecting bacterio-opsin gene expression. Nucleic Acids Res. **12:**7949–7959.
7. **Bieszke, J. A., E. N. Spudich, K. L. Scott, K. A. Borkovich, and J. L. Spudich.** 1999. A eukaryotic protein, NOP-1, binds retinal to form an archaeal rhodopsin-like photochemically reactive pigment. Biochemistry **38:**14138–14145.
8. **Bogomolni, R. A., and J. L. Spudich.** 1982. Identification of a third rhodopsin-like pigment in phototactic *Halobacterium halobium*. Proc. Natl. Acad. Sci. USA **79:**6250–6254.
9. **Botella, J. A., F. J. Murillo, and R. Ruiz-Vazquez.** 1995. A cluster of structural and regulatory genes for light-induced carotenogenesis in *Myxococcus xanthus*. Eur. J. Biochem. **233:**238–248.
10. **Britton, G.** 1985. General carotenoid methods. Methods Enzymol. **111:**113–149.
11. **Cline, S. W., W. L. Lam, R. L. Charlebois, L. C. Schalkwyk, and W. F. Doolittle.** 1989. Transformation methods for halophilic archaebacteria. Can. J. Microbiol. **35:**148–152.
12. **Dale, H., C. M. Angevine, and M. P. Krebs.** 2000. Translocation order of the extracellular domains of bacterioopsin *in vivo*. Proc. Natl. Acad. Sci. USA **97:**7847–7852.
13. **Dale, H., and M. P. Krebs.** 1999. Membrane insertion kinetics of a protein domain *in vivo*: the bacterioopsin N terminus inserts co-translationally. J. Biol. Chem. **274:**22693–22698.
14. **DasSarma, S., U. L. RajBhandary, and H. G. Khorana.** 1984. Bacterio-opsin mRNA in wild-type and bacterio-opsin-deficient *Halobacterium halobium* strains. Proc. Natl. Acad. Sci. USA **81:**125–129.
15. **Deshpande, A., and S. Sonar.** 1999. Bacterioopsin-triggered retinal biosynthesis is inhibited by bacteriorhodopsin formation in *Halobacterium salinarium*. J. Biol. Chem. **274:**23535–23540.
16. **Holmes, M. L., and M. L. Dyall-Smith.** 1990. A plasmid vector with a selectable marker for halophilic archaebacteria. J. Bacteriol. **172:**756–761.
17. **Isenbarger, T. A., and M. P. Krebs.** 1999. Role of helix-helix interactions in assembly of the bacteriorhodopsin lattice. Biochemistry **38:**9023–9030.
18. **Isenbarger, T. A., and M. P. Krebs.** 2001. Thermodynamic stability of the bacteriorhodopsin lattice as measured by lipid dilution. Biochemistry **40:**11923–11931.
19. **Krebs, M. P., T. Hauss, M. P. Heyn, U. L. RajBhandary, and H. G. Khorana.** 1991. Expression of the bacterioopsin gene in *Halobacterium halobium* using a multicopy plasmid. Proc. Natl. Acad. Sci. USA **88:**859–863.
20. **Krebs, M. P., and T. A. Isenbarger.** 2000. Structural determinants of purple membrane assembly. Biochim. Biophys. Acta **1460:**15–26.
21. **Krogh, A., B. Larsson, G. von Heijne, and E. L. L. Sonnhammer.** 2001. Predicting transmembrane protein topology with a hidden Markov model: application to complete genomes. J. Mol. Biol. **305:**567–580.
22. **Krubasik, P., and G. Sandmann.** 2000. A carotenogenic gene cluster from *Brevibacterium linens* with novel lycopene cyclase genes involved in the synthesis of aromatic carotenoids. Mol. Gen. Genet. **263:**423–432.
23. **Kushwaha, S. C., M. Kates, and J. W. Porter.** 1976. Enzymatic synthesis of C_{40} carotenes by cell-free preparation from *Halobacterium cutirubrum*. Can. J. Biochem. **54:**816–823.
24. **Lam, W. L., and W. F. Doolittle.** 1989. Shuttle vectors for the archaebacterium *Halobacterium volcanii*. Proc. Natl. Acad. Sci. USA **86:**5478–5482.
25. **Misawa, N., S. Kajiwara, K. Kondo, A. Yokoyama, Y. Satomi, T. Saito, W. Miki, and T. Ohtani.** 1995. Canthaxanthin biosynthesis by the conversion of methylene to keto groups in a hydrocarbon β-carotene by a single gene. Biochem. Biophys. Res. Commun. **209:**867–876.
26. **Ng, W. V., S. P. Kennedy, G. G. Mahairas, B. Berquist, M. Pan, H. D. Shukla, S. R. Lasky, N. S. Baliga, V. Thorsson, J. Sbrogna, S. Swartzell, D. Weir, J. Hall, T. A. Dahl, R. Welti, Y. A. Goo, B. Leithauser, K. Keller, R. Cruz, M. J. Danson, D. W. Hough, D. G. Maddocks, P. E. Jablonski, M. P. Krebs, C. M. Angevine, H. Dale, T. A. Isenbarger, R. F. Peck, M. Pohlschroder, J. L. Spudich, K. W. Jung, M. Alam, T. Freitas, S. Hou, C. J. Daniels, P. P. Dennis, A. D. Omer, H. Ebhardt, T. M. Lowe, P. Liang, M. Riley, L. Hood, and S. DasSarma.** 2000. Genome sequence of *Halobacterium* species NRC-1. Proc. Natl. Acad. Sci. USA **97:**12176–12181.
27. **Oesterhelt, D.** 1998. The structure and mechanism of the family of retinal proteins from halophilic archaea. Curr. Opin. Struct. Biol. **8:**489–500.
28. **Oesterhelt, D., and W. Stoeckenius.** 1974. Isolation of the cell membrane of *Halobacterium halobium* and its fractionation into red and purple membrane. Methods Enzymol. **31:**667–678.
29. **Peck, R. F., S. DasSarma, and M. P. Krebs.** 2000. Homologous gene knockout in the archaeon *Halobacterium salinarum* with *ura3* as a counterselectable marker. Mol. Microbiol. **35:**667–676.
30. **Peck, R. F., C. Echavarri-Erasun, E. A. Johnson, W. V. Ng, S. P. Kennedy, L. Hood, S. DasSarma, and M. P. Krebs.** 2001. *brp* and *blh* are required for synthesis of the retinal cofactor of bacteriorhodopsin in *Halobacterium salinarum*. J. Biol. Chem. **276:**5739–5744.
31. **Sapienza, C., and W. F. Doolittle.** 1982. Unusual physical organization of the *Halobacterium* genome. Nature **295:**384–389.
32. **Schmidhauser, T. J., F. R. Lauter, M. Schumacher, W. Zhou, V. E. Russo, and C. Yanofsky.** 1994. Characterization of *al-2*, the phytoene synthase gene of *Neurospora crassa*. Cloning, sequence analysis, and photoregulation. J. Biol. Chem. **269:**12060–12066.
33. **She, Q., R. K. Singh, F. Confalonieri, Y. Zivanovic, G. Allard, M. J. Awayez, C. C. Chan-Weiher, I. G. Clausen, B. A. Curtis, A. De Moors, G. Erauso, C.**

Fletcher, P. M. Gordon, I. Heikamp-de Jong, A. C. Jeffries, C. J. Kozera, N. Medina, X. Peng, H. P. Thi-Ngoc, P. Redder, M. E. Schenk, C. Theriault, N. Tolstrup, R. L. Charlebois, W. F. Doolittle, M. Duguet, T. Gaasterland, R. A. Garrett, M. A. Ragan, C. W. Sensen, and J. Van der Oost. 2001. The complete genome of the crenarchaeon *Sulfolobus solfataricus* P2. Proc. Natl. Acad. Sci. USA **98:**7835–7840.

34. **Spudich, E. N., S. A. Sundberg, D. Manor, and J. L. Spudich.** 1986. Properties of a second sensory receptor protein in *Halobacterium halobium* phototaxis. Proteins **1:**239–246.
35. **Spudich, J. L., C.-S. Yang, K.-H. Jung, and E. N. Spudich.** 2000. Retinylidene proteins: structures and functions from archaea to humans. Annu. Rev. Cell Dev. Biol. **16:**365–392.
36. **Sumper, M., and G. Herrmann.** 1976. Biosynthesis of purple membrane: control of retinal synthesis by bacterio-opsin. FEBS Lett. **71:**333–336.
37. **Sumper, M., H. Reitmeier, and D. Oesterhelt.** 1976. Biosynthesis of the purple membrane of halobacteria. Angew Chem. Int. **15:**187–194.
38. **Thompson, J. D., D. G. Higgins, and T. J. Gibson.** 1994. CLUSTAL W: improving the sensitivity of progressive multiple sequence alignment through sequence weighting, position-specific gap penalties and weight matrix choice. Nucleic Acids Res. **22:**4673–4680.
39. **Velayos, A., A. P. Eslava, and E. A. Iturriaga.** 2000. A bifunctional enzyme with lycopene cyclase and phytoene synthase activities is encoded by the *carRP* gene of *Mucor circinelloides*. Eur. J. Biochem. **267:**5509–5519.
40. **Verdoes, J. C., K. P. Krubasik, G. Sandmann, and A. J. van Ooyen.** 1999. Isolation and functional characterisation of a novel type of carotenoid biosynthetic gene from *Xanthophyllomyces dendrorhous*. Mol. Gen. Genet. **262:** 453–461.
41. **Viveiros, M., P. Krubasik, G. Sandmann, and M. Houssaini-Iraqui.** 2000. Structural and functional analysis of the gene cluster encoding carotenoid biosynthesis in *Mycobacterium aurum* A+. FEMS Microbiol. Lett. **187:**95–101.